NAP1 Modulates Binding of Linker Histone H1 to Chromatin and Induces an Extended Chromatin Fiber Conformation*⒮

J. Felix Kepert, Jacek Mazurkiewicz, Gerrit L. Heuvelman, Katalin Fejes Tóth, and Karsten Rippe[1]

From the Kirchhoff-Institut für Physik, Molecular Biophysics Group, Ruprecht-Karls-Universität Heidelberg, Im Neuenheimer Feld 227, D-69120 Heidelberg, Germany

NAP1 (<u>n</u>ucleosome <u>a</u>ssembly <u>p</u>rotein 1) is a histone chaperone that has been described to bind predominantly to the histone H2A·H2B dimer in the cell during shuttling of histones into the nucleus, nucleosome assembly/remodeling, and transcription. Here it was examined how NAP1 interacts with chromatin fibers isolated from HeLa cells. NAP1 induced a reversible change toward an extended fiber conformation as demonstrated by sedimentation velocity ultracentrifugation experiments. This transition was due to the removal of the linker histone H1. The H2A·H2B dimer remained stably bound to the native fiber fragments and to fibers devoid of linker histone H1. This was in contrast to mononucleosome substrates, which displayed a NAP1-induced removal of a single H2A·H2B dimer from the core particle. The effect of NAP1 on the chromatin fiber structure was examined by scanning/atomic force microscopy. A quantitative image analysis of ~36,000 nucleosomes revealed an increase of the average internucleosomal distance from 22.3 ± 0.4 to 27.6 ± 0.6 nm, whereas the overall fiber structure was preserved. This change reflects the disintegration of the chromatosome due to binding of H1 to NAP1 as chromatin fibers stripped from H1 showed an average nucleosome distance of 27.4 ± 0.8 nm. The findings suggest a possible role of NAP1 in chromatin remodeling processes involved in transcription and replication by modulating the local linker histone content.

The dynamic organization of chromatin in the eukaryotic nucleus is tightly connected to transcription (1–3). Transcribed chromatin is thought to be in a more open conformation with a higher accessibility to DNase I or micrococcal nuclease (4–7). On the other hand, highly compacted and dense chromatin regions, referred to as heterochromatin, are often transcriptionally inactive and contain a reduced number of genes (3, 7, 8). Several factors have been identified that promote a transition between a transcriptionally active and a more dense/inactive chromatin conformation. These include linker histones (9–11), DNA methylation (2, 12), histone modifications (13–15), and the incorporation of histone variants (16–19). The dynamic nature of chromatin manifests itself by continuous rearrangements of its three-dimensional structure. These changes involve the activity of histone chaperones that mediate the ordered deposition and the removal and exchange of histones (20–23). The central carrier of the histone H2A·H2B dimer in the cell is NAP1 (<u>n</u>ucleosome <u>a</u>ssembly <u>p</u>rotein 1) (24). NAP1 is involved in the transport of the histone H2A·H2B dimer from the cytoplasm to the nucleus and the deposition of histones onto the DNA as described in several reviews (20–23). NAP1 and other histone chaperones stimulate the binding of transcription factors to chromatin templates (25, 26). In yeast, loss of NAP1 leads to an altered gene expression of about 10% of the genome (27), and several lines of evidence suggest that NAP1 has activities related to transcription. First, it has been shown that NAP1 is present in complexes with SWR1, which catalyzes the substitution of the nucleosomal H2A·H2B dimer against the variant H2A.Z·H2B dimer (18). In addition, it has been demonstrated that NAP1 is capable of removing H2A·H2B dimers from mononucleosomes and exchanging these with the histone variant H2A.Z·H2B (28), the incorporation of which has important effects on gene expression *in vivo* (29). Second, Ito *et al.* (30) showed that upon histone acetylation of nucleosomal arrays with p300, H2A·H2B dimers are transferred to NAP1 in the presence of the transcriptional activator protein GalVP16. Third, the transcription by RNA polymerase II is facilitated by elongation factors like the FACT complex that possess histone chaperone activity (19, 31–33). As NAP1 is similar to FACT in its affinity to the H2A·H2B dimer while being present at much higher concentrations, it has been proposed to play a role in remodeling nucleosomes at the promoter or during elongation (34). Recently, a new link between NAP1 and the linker histones has been emerged. It has been shown that NAP1 acts as a linker histone chaperone in *Xenopus* eggs (35). In addition, the NAP1-related protein nucleoplasmin is capable of extracting linker histones from chromatin (36).

Despite its obvious importance to gene expression, the direct effect of NAP1 on the chromatin fiber conformation has not been characterized. In particular, it is not clear if NAP1 alone is sufficient for the extraction of the histone H2A·H2B dimer from the nucleosome in the context of the chromatin fiber as it has been reported for a mononucleosomal template (28). Because the protein composition of native chromatin fibers is complex, a variety of potential interaction partners for NAP1 exists. In particular, an interaction with linker histones has to be considered based on recent reports (35, 36). Furthermore, structural changes due to NAP1 binding to chromatin cannot be excluded.

Here the influence of NAP1 on the chromatin conformation and protein composition was investigated by analytical ultracentrifugation (AUC),[2] scanning/atomic force microscopy, and biochemical methods. AUC experiments describe the unperturbed, global conformation of chromatin fibers under physiological conditions (37–46), and SFM allows it to identify changes of the fiber geometry at the single nucleosomal level (47–57). By using a combination of these two biophysical techniques in conjunction with biochemical characterizations, it is

⒮ The on-line version of this article (available at http://www.jbc.org) contains supplemental Fig. S1.
[1] To whom correspondence should be addressed. Tel.: 49-6221-549270; Fax: 49-6221-549112; E-mail: Karsten.Rippe@kip.uni-heidelberg.de.

[2] The abbreviations used are: AUC, analytical ultracentrifugation; H1, linker histone H1; SFM, scanning force microscopy; *s*, sedimentation coefficient; nt, nucleotide; MNase, micrococcal nuclease.

shown here that NAP1 mediates the reversible removal of the linker histones from chromatin fibers. This process does not disrupt the overall fiber organization but causes a more open structure due to an increase in the average distance between two nucleosomes. These observations suggest new potential role for NAP1 in the establishment of a transcriptionally active chromatin conformation.

EXPERIMENTAL PROCEDURES

Preparation of Chromatin Fibers, NAP1, and Histones—HeLa cells were grown in RPMI (PAA Laboratories, Pasching, Austria) supplemented with 10% fetal calf serum. Cells were washed twice with an isotonic Tris-HCl buffer (IT) containing 25 mM Tris-HCl, pH 7.5, 137 mM NaCl, 5 mM KCl, 0.3 mM Na_2HPO_4, 0.5 mM $MgCl_2$, and 0.7 mM $CaCl_2$, detached from the surface using a cell scraper, and collected in IT buffer. Nonidet P-40 was added to a final concentration of 0.2% to dissolve the cell membrane. Cells were incubated on ice for 90 s and gently vortexed for 30 s four times. The nuclei were pelleted by centrifugation, resuspended in IT buffer supplemented with 50% glycerol, and frozen at −80 °C. Chromatin fiber extraction from the HeLa nuclei was conducted as described using MNase (Worthington) concentrations of 0.045 units/350 μg of chromatin for 5 min at 37 °C or 0.3 units/350 μg of chromatin for 30 min at 0 °C (58). The digestion was stopped by the addition of EDTA to a final concentration of 10 mM. The cell nuclei were sedimented, and the soluble chromatin fiber fraction in the supernatant was used for further experiments. Linker histone depletion was conducted essentially as described previously (47). The monovalent salt concentration of the fiber preparation was raised with sodium chloride to 0.35 M followed by incubation for 2 h on ice. Chromatin was loaded on a Sepharose CM 25 fast flow column equilibrated in 10 mM Tris, pH 7.5, 0.35 M NaCl, 1 mM EDTA. Flow-through fractions containing the chromatin fibers were collected, checked on 15% SDS-PAGE, and dialyzed against 10 mM Tris, pH 7.5, 50 mM KCl, 1 mM EDTA overnight at 4 °C. Recombinant histones were overexpressed, purified, and fluorescently labeled with either Alexa Fluor 488 or 633 C5 maleimide (Molecular Probes Europe BV, Leiden, Netherlands) as described previously (59, 60). Recombinant mononucleosomes were reconstituted by salt dialysis using a 146-bp DNA template containing the *Xenopus borealis* 5 S RNA positioning sequence (59) and histone H2A12C labeled with the Alexa 488 fluorophore referred to as $H2A^f$. Linker histone H1 from *Bos tauris* was purchased from Roche Diagnostics and purified as described previously (59). Histone H1 was labeled at the N terminus by mixing with Alexa Fluor 488 carboxylic acid and 2,3,5,6-tetraflourophenyl ester at molar stoichiometry in 20 mM Hepes, pH 8.0, followed by incubation at 20 °C for 1 h. Further purification with Bio-Rex 70 resin was conducted as described previously (60, 61). Labeled H1 was dialyzed against water and concentrated. Yeast NAP1 with an N-terminal His tag was overexpressed in *Escherichia coli* from plasmid pET28-yNAP1 and purified as described (60). Total RNA was extracted and purified as described previously from HeLa cells (62) and was kindly provided by Olaf Thürigen. The two most prominent bands are 18 S and 28 S rRNA of ≈2000 and ≈5000 nt long, respectively.

Analytical Ultracentrifugation—AUC experiments were carried out on a Beckman Instruments Optima XL-A with absorbance optics. The sedimentation velocity data for the chromatin samples were recorded at 20 °C in a buffer containing 10 mM Hepes, pH 8.0, 50 mM potassium acetate, 10 mM EDTA, and 0.6% (v/v) glycerol. Data were acquired at 260 nm, with a radial step size of 0.003 cm and 15,000 rpm in continuous scan mode. A partial specific volume of $\bar{\nu}$ = 0.644 ml·g^{-1} at 20 °C was calculated for the HeLa chromatin fibers from values of 0.746 ml·g^{-1} (histones) and 0.55 ml·g^{-1} (DNA) and the relative molecular weight

fractions. The molecular weight of one chromatosome unit comprises DNA (126.7 kDa) for an average nucleosome repeat length of 192 bp in HeLa cells (7), the histone octamer (108.5 kDa), and the linker histone H1 (~24 kDa). This corresponds to an extinction coefficient of ϵ_{260} = 2,514,550 M^{-1}·cm^{-1} per chromatosome calculated with an ϵ_{260} = 6500 M^{-1}·cm^{-1} per DNA nucleotide (ϵ_{260} = 2,496,000 M^{-1}·cm^{-1} for a 192-bp DNA duplex), ϵ_{260} = 17,200 M^{-1}·cm^{-1} for the histone octamer, and ϵ_{260} = 1350 M^{-1}·cm^{-1} for linker histone H1. The buffer density of ρ = 1.004 g·ml^{-1} and the viscosity η = 1.023 mPa/s at 20 °C were calculated with SEDNTERP version 1.05 by J. Philo, D. Hayes, and T. Laue (www.jphilo.mailway.com/download.htm) (see Ref. 63). Velocity sedimentation data were plotted with the program dc/dt+ version 1.16 by J. Philo (64). Sedimentation coefficients were determined with SEDPHAT version 2.0 (www.analyticalultracentrifugation.com) (65). Sedimentation equilibrium experiments were analyzed with the program Ultrascan 6.2 by B. Demeler (www.ultrascan.uthscsa.edu/). For the AUC experiments, chromatin samples were diluted with a buffer containing 10 mM Hepes, pH 8.0, 50 mM potassium acetate, and 10 mM EDTA to an absorbance of $A_{260} \approx 1$ (0.4 μM nucleosome). Where indicated, NAP1 was added to the chromatin fiber sample at concentrations of 2.4 or 3.5 μM monomer, corresponding to a ratio of about 0.75 and 1.1 NAP1 per core histone. Three different samples of NAP1 and chromatin fibers were analyzed by AUC as follows. (i) NAP1 was added directly to the chromatin fiber preparation. (ii) Chromatin fibers were preincubated with NAP1 for 1 h on ice. The histone H1 was then titrated to a concentration of 1 histone H1/2–3 NAP1. (iii) NAP1 was incubated with chromatin fibers for 1 h on ice followed by a stepwise titration of H2A·H2B dimer to a ratio of 1 histone/1 NAP1.

The complexes of $H1^f$ with NAP1 were characterized with sedimentation velocity and equilibrium experiments. $H1^f$ was mixed with NAP1 at a monomer ratio of 1:2 in 10 mM Tris, pH 7.5, 10 mM KCl, and data were recorded at 494 nm for sedimentation velocity runs and 494 and 280 nm in sedimentation equilibrium experiments.

Gel Electrophoretic Analysis of NAP1-Histone Interactions—The relative $H2A^f$·H2B dimer binding affinities of NAP1 and RNA were compared. $H2A^f$·H2B dimer was preincubated with NAP1 at a molar ratio of 1 NAP1 monomer/histone monomer in 15 mM Tris-HCl, pH 7.5, 50 mM KCl, 3% glycerol, and 0.33 mM dithiothreitol. NAP1 binds the $H2A^f$·H2B dimer with a nanomolar dissociation constant at a stoichiometry of 1 NAP1 monomer/histone (60, 66). Increasing amounts of RNA were titrated to the NAP1-$H2A^f$·H2B complex (ranging from 39 to 1560 ng), and transfer of the dimer was analyzed on 1% agarose gels. Bands were visualized by illumination with a UV light box at 302 nm and detection by a CCD camera exploiting the $H2A^f$ fluorescence. To follow the removal of histone H2A·H2B dimer from the nucleosome, reconstituted mononucleosomes (~200 nM) containing labeled $H2A^f$·H2B dimer were incubated with different NAP1 (from 0.9 to 5.1 μM) or RNA (from 7.8 to 57 ng/μl) concentrations for 2–4 h at room temperature and were analyzed by gel shift experiments. The binding stoichiometry between histone H1 and NAP1 was determined by titrating a 1 μM histone $H1^f$ solution in 10 mM Tris, pH 7.5, 36 mM KCl with increasing amounts of NAP1 (0–4 μM). The relative affinities of H2A·H2B dimer and H1 for NAP1 were compared by titrating a saturated NAP1-$H2A^r$·H2B dimer complex ($H2A^r$, Alexa 633 labeled H2A) with increasing concentrations of $H1^f$. The competitive binding of $H2A^r$·H2B and $H1^f$ to NAP1 was analyzed on 1% agarose gels as described above.

Biochemical Characterization of Chromatin Fibers—To determine which proteins were displaced by NAP1 from chromatin, 20 μl of chromatin with an absorbance of A_{260} = 3.6 (~1.5 μM nucleosomes) was incubated with 13 μM NAP1 for 3 h at room temperature and then

centrifuged for 90 min at 13,000 rpm and 20 °C in a tabletop centrifuge. The pellet was resuspended in 2× SDS loading buffer. The proteins of the supernatant were precipitated with 15% trichloroacetic acid for 30 min on ice and centrifuged at 13,000 rpm for 15 min at 4 °C. The pellet was washed with acetone, air-dried, and resuspended in 2× SDS loading buffer. Samples were analyzed on 15% SDS-PAGE. For MNase digestions, native and H1-depleted chromatin was prepared as described above. Fibers at a concentration of $A_{260} = 6$ were supplemented with 3 mM $CaCl_2$ and digested with 0.1 unit/μl MNase at 37 °C for various time points. The reaction was stopped by the addition of EDTA and SDS. Proteins were digested by proteinase K, and DNA was phenol/chloroform-extracted, ethanol-precipitated, and analyzed on 6% native polyacrylamide gels. For NAP1-treated fibers, chromatin at a nucleosome concentration of ~2.7 μM was incubated with ~23 μM NAP1 for 3 h at room temperature before digestion with MNase.

SFM Imaging and Data Analysis—SFM imaging of air-dried samples was conducted with a Nanoscope IV Multimode SFM from Veeco Instruments in "tapping mode" as described previously (59). As free NAP1 bound efficiently to the mica surface and obscured the imaging, it was removed by passing the sample through a 1-ml Bio-Spin 50 microcolumn (Bio-Rad) filled with nickel-nitrilotriacetic acid-agarose (Qiagen, Hildesheim, Germany) and equilibrated with 10 mM Hepes, pH 8.0, 50 mM potassium acetate. Directly before imaging, the eluate was diluted in the same buffer to a final concentration of $A_{260} \approx 0.02$, and 10 μl was pipetted on freshly cleaved mica. The mica was washed with distilled water and dried with nitrogen flow. The control chromatin fibers were purified and deposited identically.

For an automatic quantitative analysis of the SFM images, algorithms were developed using MATLAB version 6.5.1 (Mathworks, Natick, MA) and the ALEX program written by C. Rivetti and M. Young (see Ref. 67). The software automatically computed the position and size of each individual nucleosome and mean width, volume, area, perimeter, and height of the whole chromatin fibers. In the air-dried images, the nucleosomes appeared as spheres of about 2 nm height. To measure the area covered by the chromatin fibers, a contour line was plotted at a height of 0.2 nm above the background (Fig. 5B). The area within this contour line was considered to belong to the chromatin fiber. From this, the area covered by the fiber was calculated. The position of the nucleosomes was determined by detecting the local height maxima inside the segmented chromatin fibers. To account for noise in the topography signal, which could obscure the identification, additional constraints were implemented. First, a threshold for minimal height of a nucleosome was set to 0.4 nm. Second, the distance between two neighboring nucleosomes had to be at least 8 nm. Third, the exact positions of the nucleosome centers were determined by taking out each nucleosome of the chromatin image and by subsequent cross-correlation with a rotated copy. With this procedure, the positions of the nucleosome centers and the total number of nucleosomes of the chromatin fiber could be identified reliably as shown in Fig. 5B. The total area occupied by the chromatin fiber (see *contour line* in Fig. 5B) was divided by the number of nucleosomes. By approximating the area occupied by a nucleosome as a circle, the average distance between nucleosomes was calculated. In addition the distance of a given nucleosome to its nearest neighboring nucleosome was determined. A total of 1063 chromatin fibers with 36,261 nucleosomes were evaluated. The data for the average distance between nucleosomes were fit to a Gaussian distribution (Fig. 5C), whereas the distribution of nearest neighbor distances d (Fig. 5D) was fitted to the product of a Gaussian and $\cos^2$
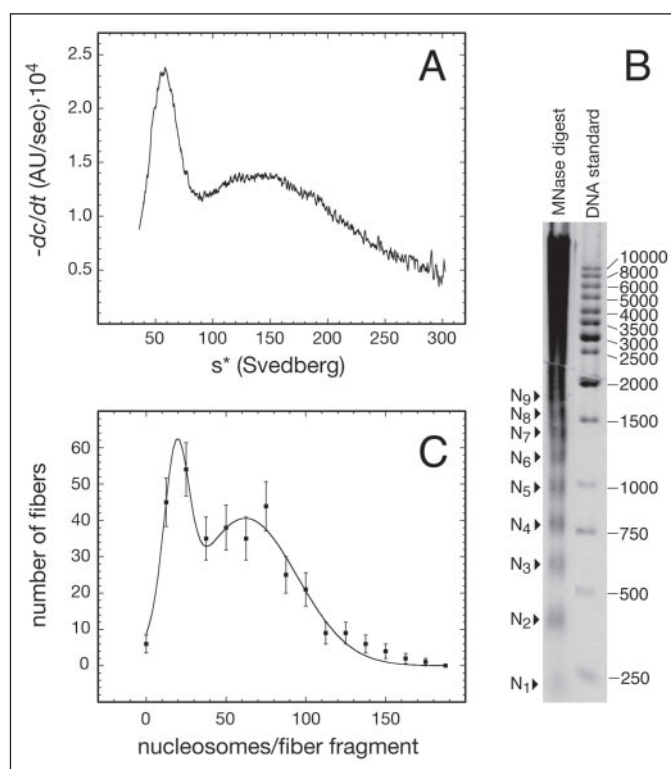

FIGURE 1. **Characterization of the chromatin fiber preparation.** *A*, distribution of sedimentation coefficients derived by the dc/dt method from AUC runs for the chromatin fiber sample studied. Averaging 11 different chromatin preparations yielded two major peaks at 46 ± 6 S and 166 ± 13 S. *B*, chromatin samples were analyzed on a 1% agarose gel after mild micrococcal nuclease digestion. The digestion pattern revealed the existence of a regular nucleosome spacing characteristic for native chromatin. DNA bands corresponding to fragments with 1–9 nucleosomes (N_1 to N_9) are marked. *C*, distribution of the number of nucleosomes per single chromatin fiber fragment determined on SFM images.

to account for the observed periodicity of peaks as shown in Equation 1.

$$p(d) = c_1 \cdot \exp\left(\frac{(d - \bar{d})^2}{2 \cdot \sigma^2}\right) \cdot (\cos^2(c_2 \cdot d + c_3) + 4) \quad \text{(Eq. 1)}$$

In Equation 1 $\bar{d}$ is the average distance between nearest neighboring nucleosomes; σ is the standard deviation, and c_1, c_2, and c_3 are constants.

RESULTS

NAP1 Reversibly Alters the Hydrodynamic Shape of Native Chromatin Fibers—Analytical ultracentrifugation was used to determine the sedimentation properties of native chromatin fibers from HeLa cells in the presence of NAP1. These fibers were analyzed by sedimentation velocity ultracentrifugation. From averaging 11 different chromatin preparations, values of $s_{20,w} = 46 \pm 6$ S and $s_{20,w} = 166 \pm 13$ S were derived for the two main peaks as shown in Fig. 1A (sedimentation coefficients ($s_{20,w}$) at standard conditions of water, 20 °C). These s values correspond to chromatin fiber fractions of different lengths. The isolated chromatin fibers were analyzed by partial MNase digestion and showed regular spacing, which demonstrates the integrity of the fiber preparation (Fig. 1B). In order to determine the length distribution of the fiber fragments, the number of nucleosomes per fiber was counted on scanning force microscopy images, and a bimodal distribution with two peaks at 19 ± 2 and 62 ± 5 nucleosomes was observed when fitted with the sum of two Gaussians (Fig. 1C). The two distributions had standard deviations of 7 and 32 nucleosomes, respectively. Previous
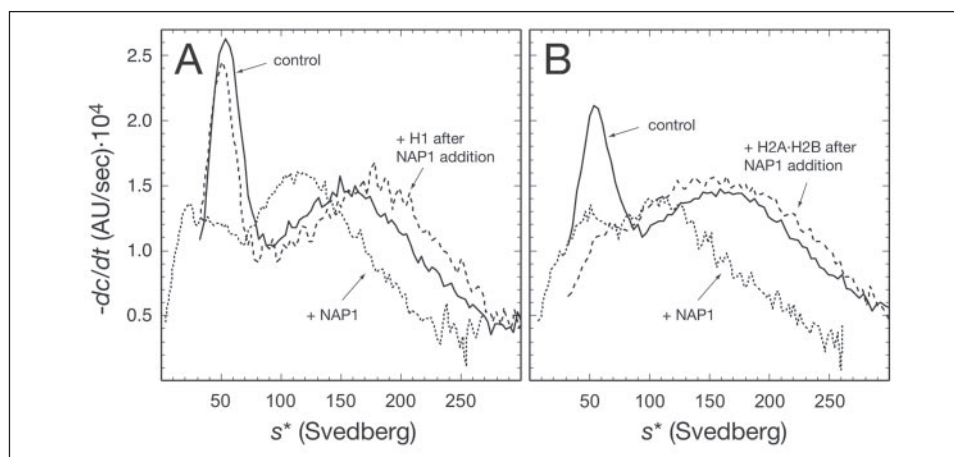
FIGURE 2. **Effect of NAP1 on the sedimentation coefficients distribution of chromatin fibers.** Representative examples for the different type of experiments are shown. All samples contained chromatin fibers at an $A_{260} \approx 1$. For the chromatin control samples, an average sedimentation distribution with two peaks at 46 ± 6 S and 166 ± 13 S was obtained. The sedimentation distribution for NAP1-incubated chromatin yielded two peaks with average values of 25 ± 3 S and 116 ± 6 S. *A* and *B*, the control chromatin fibers are shown as *solid lines*, the fibers incubated with NAP1 as *dotted lines,* and the NAP1 incubated fibers that were either titrated with H1 or H2A·H2B dimer as *dashed lines*. *A*, chromatin fibers were incubated with NAP1 at a concentration of 2.4 μM for 2 h. Then histone H1 was added in small aliquots to an end concentration of 0.8 μM. The resulting sedimentation distribution displayed two peaks with average values of 40 ± 3 S and 160 ± 16 S. *B*, chromatin fibers that were preincubated with 3.5 μM NAP1 were titrated stepwise to a final concentration of 1.7 μM H2A·H2B dimer. The distribution at the titration end point had two peaks with average values of 40 ± 7 S and 157 ± 19 S.

work showed that chromatin fibers with ~20 and 45 nucleosomes have a sedimentation coefficient of ~50 and 110 S under similar salt concentrations (68). As the number of nucleosomes measured by SFM is in excellent agreement with these results, the 50 S peak could be assigned to chromatin fiber fragments with ~20 nucleosomes and the 160 S species to chromatin fibers with ~60 nucleosomes.

To examine the effect of NAP1 on chromatin conformation, isolated fibers were preincubated with NAP1 for at least 1 h on ice and subsequently analyzed by sedimentation velocity experiments. As shown in Fig. 2, *A* and *B*, the sedimentation profile changes dramatically upon incubation with NAP1. The sedimentation coefficients of the main species were significantly shifted to lower *s* values, and two maxima at 25 ± 3 and 116 ± 6 S ($n = 4$ experiments) were obtained. This corresponds to a 45 and 30% decrease of the sedimentation coefficients for the two peaks, as compared with the control chromatin fibers. The peak at around 25 S was also reduced in height, indicating that the total amount of molecules with this sedimentation coefficient was decreased. The changes in the sedimentation profile could be reversed by the addition of either H1 (Fig. 2*A*) or H2A·H2B dimer (Fig. 2*B*). The two main peaks in the sedimentation coefficient profile were found at 40 ± 3 and 160 ± 16 S upon addition of H1 ($n = 4$ experiments, Fig. 2*A*) and at 40 ± 7 and 157 ± 19 S after titration with H2A·H2B dimer ($n = 3$ experiments, Fig. 2*B*).

NAP1 Removes the Linker Histone H1 from Native Fibers Leaving the Nucleosome Core Unaltered—To identify which histone proteins were displaced by NAP1, the protein composition was determined after separating the chromatin fibers from NAP1 by centrifugation (Fig. 3A). NAP1 induced the transition of histone H1 from the chromatin-containing pellet to the NAP1-containing supernatant. No core histones were found in the NAP1-containing supernatant, indicating that the core histones were not displaced by NAP1 from the chromatin fiber. The same experiments were also conducted with chromatin fibers that were depleted of linker histone H1. The stripped fibers also showed no significant displacement of core histone proteins from chromatin (Fig. 3*A*, *lane 13*). Only very small amounts of histone H2A·H2B dimer were found in the NAP1-containing fraction. Thus, NAP1 removes the linker histone H1 from native chromatin fibers and does not mobilize significant amounts of the core histones.

To analyze whether NAP1 alters the nucleosome spacing or the length of DNA protected by the nucleosome, MNase digestions were performed (supplemental Fig. S1). Upon NAP1 incubation, a single DNA band of ~146 bp was visible indicating the displacement of linker histones from chromatin.

NAP1 and RNA Mediated H2A·H2B Dimer Extraction—Because NAP1 was not able to extract significant amounts of core histones from native chromatin fibers, it was analyzed whether NAP1 can remove the H2A·H2B dimer from reconstituted mononucleosomes. Gel shift experiments were conducted with mononucleosomes containing fluorescently labeled histone H2A. In addition, RNA as a high affinity but bona fide unspecific histone binding partner was used to extract histone dimers from the mononucleosomes. The NAP1-H2A^f·H2B or RNA-H2A^f·H2B complexes were clearly separated from the mononucleosome band on standard agarose gels allowing the visualization of the transfer of H2A^f·H2B dimers from nucleosomes into a complex with NAP1 or RNA (Fig. 3*B*). To determine the relative binding affinities of NAP1 and RNA to the H2A^f·H2B dimer, the NAP1-H2A^f·H2B complex was titrated with increasing amounts of RNA (Fig. 3*B*, *lanes 1–7*). A competition with RNA for H2A^f·H2B in complex with NAP1 was evident, and equivalent concentrations of RNA and NAP1 were determined. Then mononucleosome solutions of about 200 nM were incubated with different amounts of NAP1 or RNA for 2–4 h at room temperature. Fig. 3*B*, *lanes 8–14*, shows the redistribution of the fluorescence signal from the mononucleosome band with increasing concentrations of NAP1 or RNA. In these experiments an additional fluorescent band was visible below the mononucleosome. This band could be assigned to a nucleosome complex with a histone hexamer core as it contained the H2A^f fluorescence, and ethidium bromide staining indicated the presence of DNA. This hexasome was the predominant species formed upon incubation of mononucleosomes with NAP1 or RNA, with some complete dissociation observed at high concentrations when using a 146-bp DNA template (Fig. 3*B*, *lane 21*). For control experiments unlabeled mononucleosomes were also incubated with NAP1, resulting in equivalent dimer extraction as similar ethidium bromide staining pattern was apparent, indicating that fluorescence labeling did not alter nucleosome stability (data not shown). Both RNA and NAP1
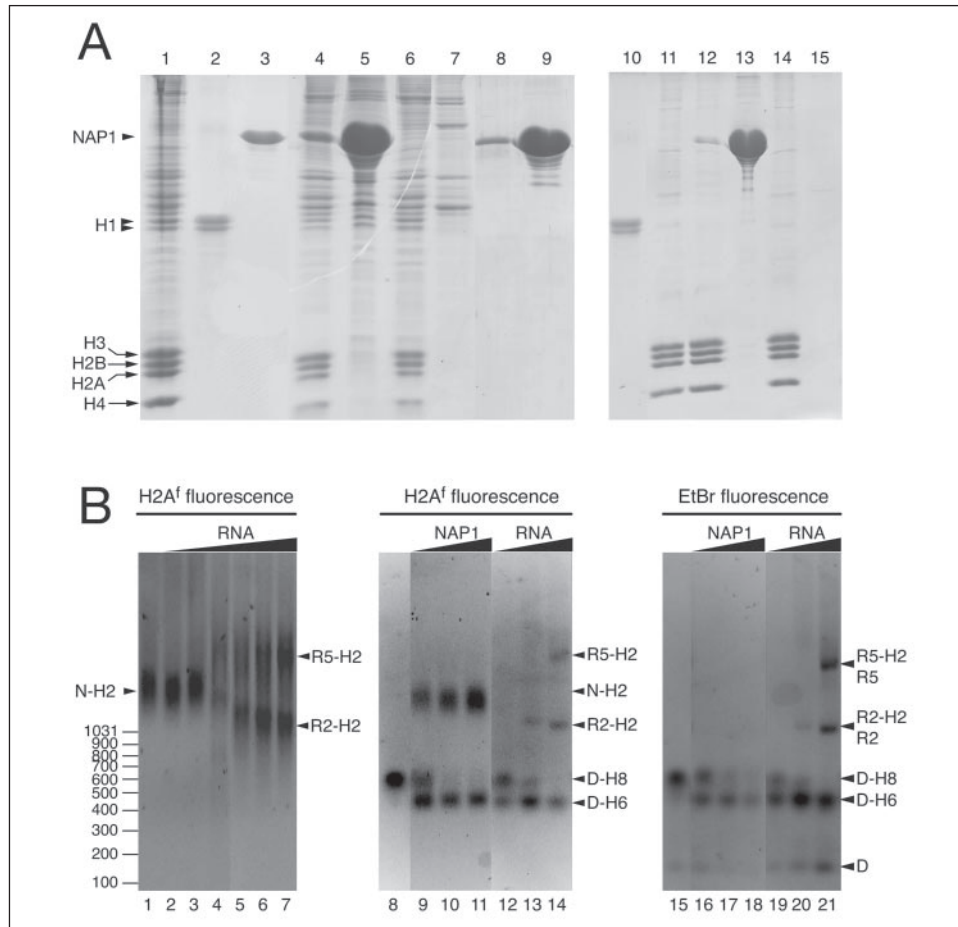
FIGURE 3. **Characterization of the proteins displaced from chromatin fiber and mononucleosomes by NAP1.** *A,* SDS-PAGE of native HeLa chromatin treated with NAP1. Chromatin was incubated with NAP1 and then pelleted to separate soluble NAP1 and interacting proteins from chromatin. *Left panel,* analysis of native chromatin fibers (*lanes 1–9*). *Lane 1,* whole chromatin sample; *lane 2,* H1; *lane 3,* NAP1; *lane 4,* pellet of chromatin incubated with NAP1; *lane 5,* supernatant of chromatin incubated with NAP1; *lane 6,* pellet of chromatin without added NAP1; *lane 7,* supernatant of chromatin without added NAP1; *lane 8,* pellet of NAP1 alone; *lane 9,* supernatant of NAP1 alone. *Right panel,* analysis of chromatin fibers that were stripped of linker histone H1 (*lanes 10–15*). *Lane 10,* H1; *lane 11,* whole H1-stripped chromatin sample; *lane 12,* pellet of chromatin incubated with NAP1; *lane 13,* supernatant of chromatin incubated with NAP1; *lane 14,* pellet of chromatin without added NAP1; *lane 15,* supernatant of chromatin without added NAP1. *B,* removal of H2A^f·H2B dimers from reconstituted mononucleosomes by NAP1 and RNA analyzed by gel electrophoresis. The following abbreviations are used to assign the bands: *D,* free 146-bp DNA; *H2,* H2A^f·H2B dimer; *D-H6,* nucleosome with histone hexamer core, where one H2A·H2B dimer is missing; *D-H8,* complete mononucleosome; *N-H2,* complex of NAP1 with H2A^f·H2B dimer; *R2,* free 18 S rRNA (≈2000 nt); *R5,* free 28 S rRNA (≈5000 nt); *R2-H2,* complex of 18 S rRNA with H2A^f·H2B dimer; *R5-H2,* complex of 28 S rRNA with H2A^f·H2B dimer. *Left panel* (*lanes 1–7*), complex of NAP1 (6 μM) and H2A^f·H2B dimer (3 μM) was titrated with increasing amounts of RNA and visualized by recording the H2A^f fluorescence. RNA concentrations: *lane 1,* no RNA; *lane 2,* 6.5 ng/μl; *lane 3,* 13 ng/μl; *lane 4,* 30 ng/μl; *lane 5,* 70 ng/μl; *lane 6,* 120 ng/μl; *lane 7,* 240 ng/μl. At increased RNA concentrations a transition of H2A^f·H2B from a NAP1-H2A^f·H2B complex into an RNA-H2A^f·H2B complex was observed. *Center panel* (*lanes 8–14*): recombinant mononucleosomes (200 nM) reconstituted with H2A^f were incubated with increasing NAP1 and RNA concentrations: *lane 8,* no NAP1 and RNA; *lane 9,* 0.9 μM NAP1; *lane 10,* 3.3 μM NAP1; *lane 11,* 5.1 μM NAP1; *lane 12,* 7.8 ng/μl RNA; *lane 13,* 18 ng/μl RNA; and *lane 14,* 58 ng/μl RNA. Samples were visualized by detection of the H2A^f fluorescence. *Right panel* (*lanes 15–21*), same sample composition as in *lanes 8–14,* but visualization of DNA bands was via ethidium bromide staining.

seemed to be similarly efficient in extracting one histone H2A^f·H2B dimer from the mononucleosome complex at the concentrations used.

Scanning Force Microscopy Analysis of Chromatin Fibers—The structural changes caused by the incubation of chromatin fibers with NAP1 were further analyzed by scanning force microscopy. As shown on the images in Fig. 4, A–D, the isolated native chromatin fibers adopted various conformational states. In contrast to other studies, these fibers were not treated by fixation agents and were deposited to the mica surface by a procedure that leads to minimal disturbance of the sample. Some of the molecules had a fiber-like structure, although others were more condensed and hence probably represent chromatin fragments that are folded beyond the 30-nm fiber. According to the chromonema model, an additional compaction of the 30-nm fiber is achieved by its folding into 60–80- and 100–130-nm chromonema fibers (69–71). Analysis of the fiber height profiles revealed that in almost all regions only a single layer of nucleosomes was present. This suggests that upon binding of the fiber to the surface, its three-dimensional organization is

rearranged so that all nucleosomes can contact the surface, in an equilibration process similar to the one that has been observed for long DNA fragments (72). Thus, the number and position of all nucleosomes present in the fiber could be determined. A total of 36,261 nucleosomes in 1063 fibers were evaluated. It is noted that the quantification of the nucleosome number per individual fiber on the SFM images agreed with the observed sedimentation behavior of the chromatin fibers (Fig. 1).

To elucidate the effects of NAP1 on the chromatin conformation, fibers incubated with NAP1 were examined. Incubation of chromatin with NAP1 did not have drastic effects on the conformation, which was apparent by simple visual inspection of the SFM images (Fig. 4, E–H). To compare with the linker histone-depleted chromatin conformation, H1-stripped chromatin fibers were imaged with the SFM. The overall folding in these fibers did not change significantly (Fig. 4, I–L). However, the quantification of the average internucleosomal distances within the chromatin fibers revealed distinct changes upon NAP1 treatment. A total of 125 control fibers (9550 nucleosomes), 753 fibers without H1

FIGURE 4. **SFM images of chromatin fibers (1 × 1 μm images).** *A–D,* single chromatin fiber fragments. *E–H,* chromatin fibers incubated with NAP1. *I–L,* chromatin fibers depleted of linker histone H1.
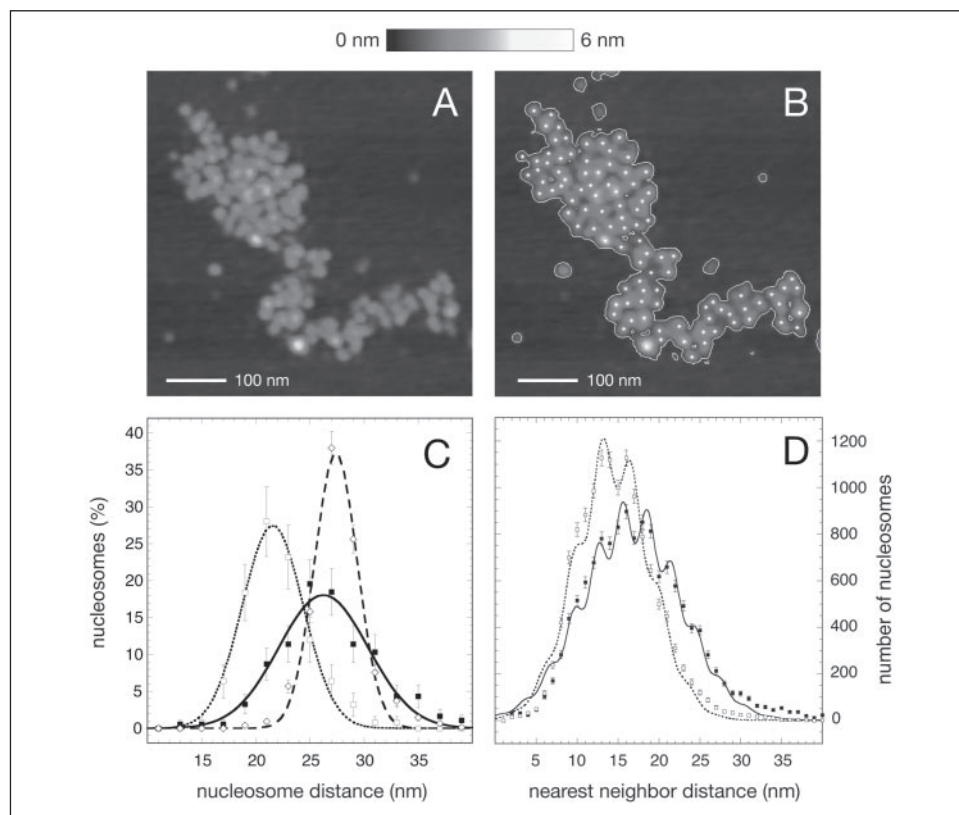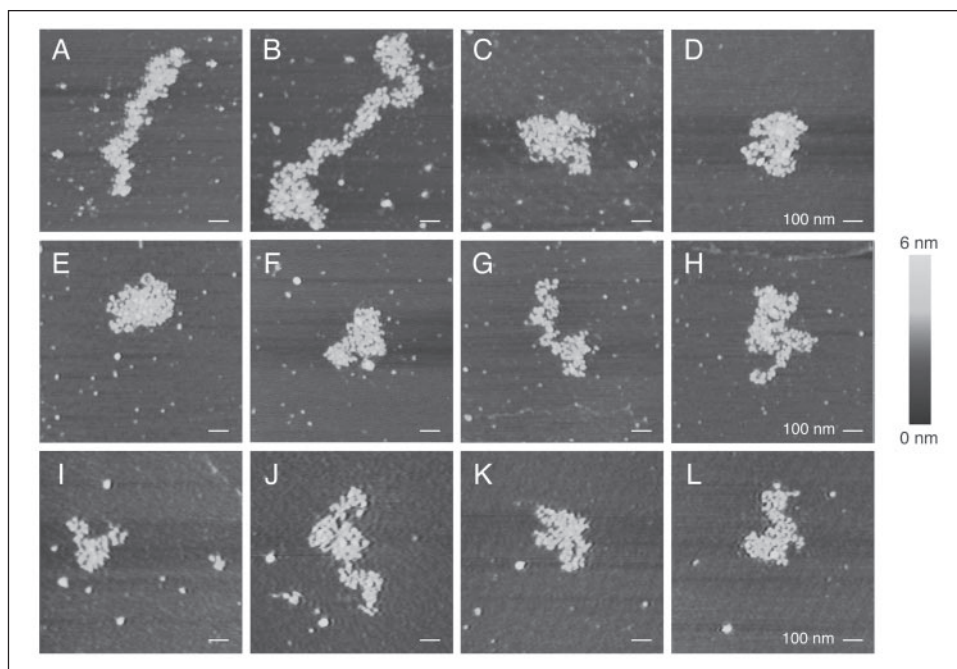

FIGURE 5. **Image analysis of chromatin fibers to determine internucleosomal distances.** *A,* original SFM image, 550 × 550 nm scan. *B,* the area of the chromatin fiber was segmented as indicated by a contour line around the fiber. Centers of the individual nucleosomes were automatically identified and are depicted in the image with *white asterisks. C,* histogram of the average internucleosomal distance within control chromatin fibers (*open squares*), chromatin fibers incubated with NAP1 (*black squares*) and fibers without H1 (*open diamonds*). The average value for the distance distribution increased from 22.3 ± 0.4 to 27.6 ± 0.6 nm upon removal of histone H1 by NAP1. In addition, the distribution of distances became broader with standard deviations of 2.5 for the control and 4.2 nm for the NAP1-treated fibers. For chromatin fibers stripped of linker histones, an average distance of 27.4 ± 0.8 nm was obtained. *D,* distribution of distances of a given nucleosome to its nearest neighbor nucleosome. Both control fibers (*open squares*) and chromatin fibers incubated with NAP1 (*black squares*) displayed peaks with a periodicity of 2.9 nm that is likely to reflect the three-dimensional folding of the nucleosome chain in the 30-nm chromatin fiber. Accordingly, the data were fitted with a modified Gaussian distribution (see Equation 1).

(13441 nucleosomes), and 184 chromatin fibers (13,280 nucleosomes) incubated with NAP1 from 4 or 5 different sample depositions were evaluated. Fig. 5*C* shows the histogram of the internucleosomal distances for control chromatin fibers, the H1-stripped fibers, and those incubated with NAP1. The average distance between the nucleosomes increased from 22.3 ± 0.4 nm for the control to 27.6 ± 0.6 nm in the presence of NAP1. The difference of 5.3 ± 0.7 nm would correspond to ~17-bp DNA released from the nucleosome. This increased nucleosomal distance is also found in the linker histone-stripped fibers that showed mean distances of 27.4 ± 0.8 nm. The distribution of the internucleosomal distances for the NAP1 incubated fibers was also broadened compared with control chromatin as apparent from the different standard deviations of 2.5 to 4.2 nm. This may be due to the increased heterogeneity in nucleosome composition of the resulting fiber. In order to characterize the organization of individual nucleosomes, the distance between a given nucleosome and its nearest neighbor was measured. The corresponding relation is shown in Fig. 5*D*. Again the whole distribution was shifted to larger distances by 2.7 nm and showed

some broadening with average values of 14.9 ± 0.1 and 17.6 ± 0.1 nm and standard deviations of 4.6 and 6.0 nm in the absence and presence of NAP1. Most interestingly, the two distributions were not of a simple Gaussian shape but showed several peaks/shoulders at about 10.4, 13.2, 16.4, and 19.4 nm for the control and at 10.0, 12.8, 15.6, 18.6, 21.4, and 24.2 nm in the presence of NAP1. This corresponds to a periodical distance of 2.9 ± 0.1 nm between peaks for the two samples. This nearest neighbor distance distribution of the surface-bound fibers reflects the three-dimensional organization of the repeating unit of the chromatin fiber, and its relation to different fiber geometries is currently being evaluated.[3] In the presence of NAP1, the periodicity of the peaks was preserved, but the distribution on an average shifted by 2.7 nm. This suggests that the overall

---

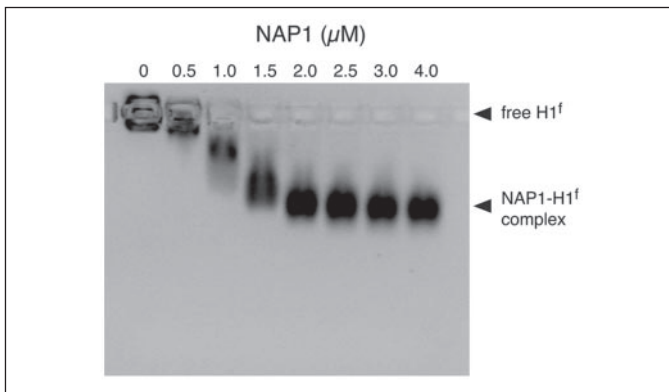[3] G. L. Heuvelman, G. Wedemann, J. F. Kepert, and K. Rippe, manuscript in preparation.

FIGURE 6. **Gel shift analysis of NAP1 with histone H1[f].** Increasing amounts of NAP1 (0.5, 1, 1.5, 2.0, 2.5, 3, and 4 μM) were mixed with 1 μM histone H1[f]. Histone H1[f] was completely shifted into a NAP1 containing complex at a concentration of 2 μM NAP1, indicating a 2:1 complex of NAP1 and histone H1.

organization of the chromatin fibers was maintained upon removal of histone H1 by NAP1, while the distance between the nucleosomes increased.

NAP1 Binds the Linker Histone H1[f] with a 2:1 Stoichiometry and with a Comparable Affinity as the H2A·H2B Dimer—By electrophoretic gel mobility shift analysis, the binding stoichiometry of NAP1 to H1[f] was determined. First histone H1[f] was titrated with increasing amounts of NAP1 showing the formation of a distinct complex at a stoichiometry of 2 ± 0.5 NAP1 monomer/histone monomer (Fig. 6). In order to compare the binding affinities of H2A·H2B dimer and H1 to NAP1, a saturated H2A[r]·H2B dimer-NAP1 complex was titrated with H1[f] (r and f = labeling with Alexa 633 and 488, respectively). H1[f] was capable of competing with histone H2A[r]·H2B dimer for NAP1 binding. Because histone H2A[r]·H2B and H1[f] were labeled with different dyes and migrated slightly different in their complexes with NAP1, the two complexes could be separated on agarose gels and visualized with UV excitation light (data not shown). H1[f] seemed to be efficient in binding to NAP1 as titrated H1[f] bound to NAP1 that was previously saturated with H2A[r]·H2B dimer.

The molecular weights and association states of the NAP1-H1[f] complexes were determined by sedimentation equilibrium experiments under low salt conditions (10 mM Tris, pH 7.5, and 10 mM KCl; see Fig. 7, *A* and *B*). Initial analysis showed that the data could only be fitted poorly to a one-component model, with a mean molecular mass between 200 and 400 kDa, indicating the presence of higher order complexes. The absorbance profiles at three different protein concentrations and two different wavelengths could be fitted most accurately with a model of a monomer-tetramer equilibrium (Fig. 7, *A* and *B*). The molecular weight for the monomer was fixed to 126 kDa during fitting, which corresponds to a complex consisting of two NAP1 and one H1[f]. The oligomerization of the NAP1$_2$-H1[f] complex in a monomer-tetramer equilibrium was further confirmed by sedimentation velocity
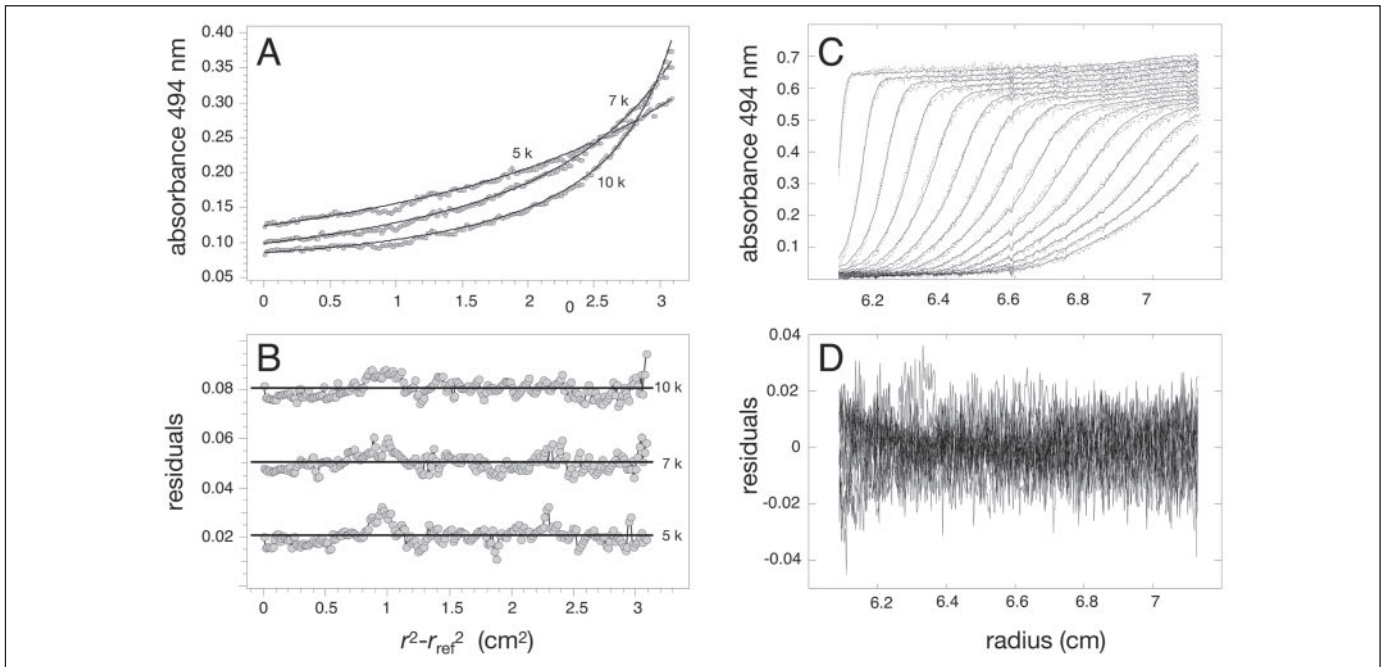

FIGURE 7. **AUC analysis of NAP1 complexes with histone H1[f].** NAP1 samples between 8 and 16 μM were mixed with histone H1[f] in a 2:1 ratio (monomer NAP1: monomer H1[f]). *A*, sedimentation equilibrium analysis of NAP1-H1[f] complexes. Data were recorded at 5000, 7000, and 10,000 rpm at 494 nm. The fits of a monomer-tetramer model to the absorbance profiles are shown by *solid lines*. The monomer represents a complex of a NAP1 dimer with one H1 and a molecular mass of 126 kDa. *B*, residuals of the fitted function to the absorbance data shown under *A*. *C*, sedimentation velocity analysis. NAP1 at 16 μM was mixed with 8 μM H1[f], and data were recorded at 494 nm, 37,000 rpm, and 20 °C in a continuous scan mode. As in *A*, a monomer-tetramer equilibrium model was fitted to the absorbance data (*solid line*, every sixth scan is shown), with a (NAP1)$_2$-H1 complex as monomer. *D*, residuals for the fit presented in *C*.

experiments. As shown in Fig. 7, *C* and *D,* the velocity sedimentation profiles could be fitted well with a monomer-tetramer model yielding sedimentation coefficients of 6.1 ± 0.1 S and 10.5 ± 1 S for the monomer and tetramer, respectively. Again the molecular mass for the monomer was fixed to 126 kDa during fitting.

DISCUSSION

NAP1 was initially described as a factor that facilitates nucleosome assembly (24). In later reports it has been also linked to other cellular processes like histone transport, gene expression, and nucleosome remodeling (18, 21, 27, 34, 73). Here we examined how NAP1 affects the chromatin fiber organization. A NAP1-induced transition to an extended fiber conformation was observed by AUC and SFM. Our results show that NAP1 binds to histone H1 with high affinity. This leads to the reversible removal of linker histones from chromatin.

The chromatin fibers studied were isolated from HeLa cells and showed hydrodynamic and structural properties comparable with earlier studies (38, 47, 58, 74). Incubation with NAP1 changed the chromatin sedimentation profile significantly as apparent from the 30–45% decrease of the sedimentation coefficient distribution. This predominantly reflects an extension of the chromatin fiber shape and to a smaller extent an up to ~10% reduction of the molecular weight because of the loss of H1. The latter effect would correspond to an equal decrease in the sedimentation coefficient if the frictional coefficient remained constant. Thus, a 20–35% reduction of the *s* value distribution was due to a change of the chromatin conformation to a more extended shape. This is consistent with previous reports on the effect of linker histone binding to chromatin where similar changes in the sedimentation coefficient have been reported (37, 75, 76). For the first maximum of around 50 S (~20 nucleosomes) some height reduction and broadening were observed in the presence of NAP1 in addition to the shift of the maximum (Fig. 2*A*). Apparently, nucleosomes are more accessible in these shorter chromatin fibers, and linker histones could be extracted more easily as compared with the second peak of the distribution at 160 S (~60 nucleosomes). This might be due to a folding of longer chromatin fibers into higher order structures of 60–130 nm diameter (69–71), in which additional internucleosomal contacts are present that could stabilize the chromatosome structure.

The additional compaction beyond the 30-nm chromatin fiber was apparent also on the SFM images. On these images the chromatin conformation changes induced by NAP1 could be examined on the single nucleosomal level. The NAP1-treated fibers retained a similar organization, and no large differences were visible from a simple inspection of the images (Fig. 4). However, quantitative analysis revealed an increase in the internucleosomal distance by about 5 nm from 22.3 ± 0.4 to 27.6 ± 0.6 nm upon incubation with NAP1. This can be explained by the partial release of DNA from the chromatosome in the DNA entry-exit region. The control with H1-stripped fibers had an average distance of 27.4 ± 0.8 nm, which further confirmed that the NAP1-induced changes were because of linker histone displacement. It has been reported previously that linker histone extraction changes the center to center distances between nucleosomes in the chromatin fiber and induces an opening of the chromatin fiber (47, 48). Most interestingly, the DNA hypermethylation of chromatin, which has been correlated with a more compact and biologically inactive conformation, induced a similar decrease of the internucleosomal distance by ~4 nm, from 28 to 24 nm, although the overall fiber conformation was also preserved (52). Thus, we conclude that the chromatin fiber organization can accommodate changes of the internucleosome distance of 4–5 nm. Such a nucleosome distance reduction appears to be characteristic for the tran-
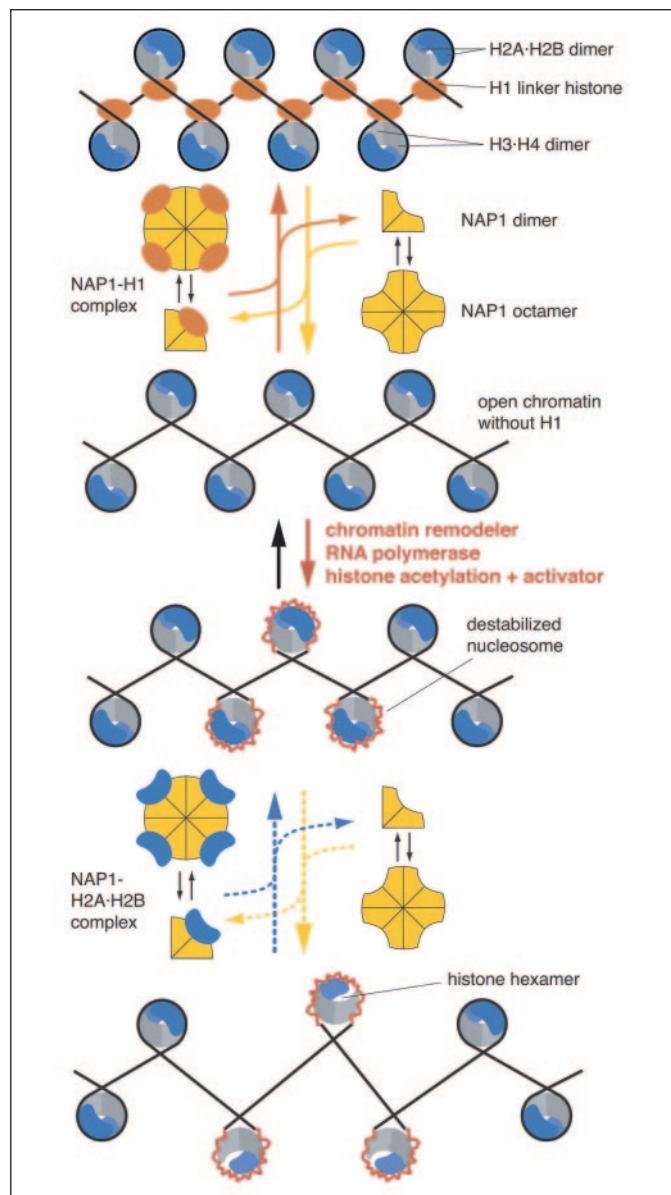

FIGURE 8. **Effects of NAP1 on the chromatin fiber conformation.** NAP1 is in a dimer-octamer equilibrium as described in a previous study (60) and binds linker histone H1 from chromatin fibers. This induces a more open and extended chromatin conformation with an increased internucleosome distance. In the absence of additional protein factors, NAP1 will not remove H2A·H2B dimer from H1-depleted fibers (Fig. 3*A*), but it can do so with mononucleosomes as described previously (28) (see also Fig. 3*B*). Furthermore, it has been reported that NAP1 is involved in H2A·H2B dimer exchange on nucleosomal arrays by the SWR1 chromatin remodeling complex (18) or in an *in vitro* system with acetylated histones and the transcriptional activator GalVP16 (30). NAP1-related histone chaperone activities have also been identified in the context of RNA polymerase II transcription where nucleosomes with a histone hexamer core form that are lacking one H2A·H2B dimer (19, 31–34, 77, 82, 83). Accordingly, a NAP1-mediated removal of one H2A·H2B dimer that requires destabilization of the nucleosome structure due, for example, to chromatin remodeling or RNA polymerase activity has been included in the scheme. As indicated by the *dashed arrows,* the occurrence of this reaction with chromatin fibers remains to be demonstrated.

sition of the chromatin fiber between transcriptionally active and more repressive conformations.

The binding stoichiometry of linker histone H1 with NAP1 and the molecular composition of the resulting complexes were analyzed by AUC and gel shift experiments. In the gel shift analysis, a binding stoichiometry of two NAP1 monomers per histone H1 monomer was observed, which was also consistent with the AUC experiments where H1 was titrated to chromatin fibers preincubated with NAP1 in order to reverse the NAP1-induced conformation changes. As inferred from the

AUC sedimentation velocity and sedimentation equilibrium experiments, a complex of one NAP1 dimer with one H1 is formed, which was in equilibrium with a complex of a NAP1 octamer associated with four H1 molecules (504 kDa). This was very similar to the association properties of NAP1 in complexes with the H2A·H2B dimer (60). In addition, Shintomi *et al.* (35) reported recently that NAP1 binds to the H1 analogue B4 in *Xenopus* egg and acts as a linker histone chaperone. The authors estimated a NAP1:B4 binding stoichiometry of 2:1 and observed that the complex of NAP1-B4 migrated in native polyacrylamide gels with an apparent molecular mass of ~230 kDa and an additional band of ~500 kDa, which is also indicative of the formation of higher order association states.

NAP1 has been related previously to histone exchange and was proposed to be involved in transcription (18, 28, 34). Transcription elongation is facilitated by factors that alter nucleosomes in order to allow RNA polymerase to proceed along the template (31, 33, 77–81). One of these factors, the FACT complex, has histone chaperone activity that facilitates the movement of RNA polymerases along the template by extracting H2A·H2B dimers from the nucleosome complexes (19, 31–33). The resulting nucleosomes with a hexameric histone core appear to be intermediates of transcription through chromatin (19, 77, 82, 83). Accordingly, histone chaperones like NAP1 have been proposed to be involved in the transient removal of the H2A·H2B dimer from the octamer, while preserving most of the overall nucleosomal structure as opposed to a complete removal and subsequent *de novo* assembly of nucleosomes (34). This activity has been demonstrated in *in vitro* experiments where NAP1 was sufficient for extracting and exchanging the H2A·H2B dimer from a mononucleosome (28). Here, we also observed that NAP1 as well as RNA are capable of extracting the H2A·H2B dimer at the mononucleosomal level. However, NAP1 failed to do so in the context of native chromatin fibers. Because RNA has a strong histone binding affinity but has not been reported to interact specifically with nucleosomes, it seems likely that both NAP1 and RNA bind histones that have already dissociated from the nucleosome (84). This process would not require a specific interaction with nucleosomes, which is in agreement with the observation that NAP1 binds H2A·H2B dimer and histone H1 tightly with dissociation constants in the nanomolar range but has low affinity to nucleosomes (60, 85). The dissociation of the H2A·H2B dimer appears to occur only at a very slow rate with chromatin fibers in the absence of additional factors. In contrast, the linker histone H1 displays a much higher mobility and exchange rate *in vivo* than the core histones as reviewed in Ref. 86.

An inhibition of transcription by linker histone H1 has been reported in a number of studies, and it is clear that the transition of chromatin to a transcriptionally active state has to involve the removal of linker histones (10, 11, 76, 87, 88). Binding to NAP1 would provide a mechanism of how this can be established. A recent study described the interaction of the acidic nuclear protein parathymosin with H1 (9). This protein has only a modest affinity for linker histone H1 with a dissociation constant in the μM range but nevertheless induces chromatin decondensation *in vivo*. Thus, it seems likely that NAP1 as a binding partner for H1 with a nanomolar dissociation constant can exert the same effect on chromatin.

In summary, we propose that NAP1 can induce a more open chromatin conformation via the pathway depicted in Fig. 8. NAP1 is present in a dimer-octamer equilibrium and can bind both H1 and the H2A·H2B dimer with high affinity as shown here and in Ref. 60. In the absence of additional factors, NAP1 will extract only linker histones from chromatin fibers. The H2A·H2B dimer remained stably bound in the nucleosomes, even if fibers devoid of H1 were examined. Thus, the removal/exchange of the H2A·H2B dimer by NAP1 observed with mononucleosomes (28) requires an additional destabilization of the chromatin fiber/nucleosome structure, possibly due to the activity of chromatin remodelers (18), RNA polymerase (34), or histone acetylation and a transcriptional activator (30). These factors could facilitate the removal of a single histone H2A·H2B dimer by NAP1 or a related histone chaperone activity to form chromatin-containing nucleosomes with a histone hexamer core that has been reported to be an intermediate of actively transcribed chromatin (19, 31–34, 77, 82, 83). On the other hand, it is demonstrated here that the high affinity binding of NAP1 and H1 occurs readily with chromatin fibers. The physiological relevance of this process is supported by the recent observation that NAP1 interacts *in vivo* with the H1 analogue B4 in *Xenopus* eggs (35). As the absence of H1 is an essential feature of transcriptionally active chromatin, the formation of a NAP1-H1 complex might be the origin for the global effects of NAP1 on gene expression (27).

REFERENCES

1. Vermaak, D., Ahmad, K., and Henikoff, S. (2003) *Curr. Opin. Cell Biol.* **15,** 266–274
2. Felsenfeld, G., and Groudine, M. (2003) *Nature* **421,** 448–453
3. Gilbert, N., Boyle, S., Fiegler, H., Woodfine, K., Carter, N. P., and Bickmore, W. A. (2004) *Cell* **118,** 555–566
4. Weintraub, H., and Groudine, M. (1976) *Science* **193,** 848–856
5. Wu, C., Wong, Y. C., and Elgin, S. C. (1979) *Cell* **16,** 807–814
6. Bellard, M., Kuo, M. T., Dretzen, G., and Chambon, P. (1980) *Nucleic Acids Res.* **8,** 2737–2750
7. van Holde, K. E. (1989) *Chromatin*, Springer-Verlag, Heidelberg
8. Dillon, N. (2004) *Biol. Cell* **96,** 631–637
9. Martic, G., Karetsou, Z., Kefala, K., Politou, A. S., Clapier, C. R., Straub, T., and Papamarcaki, T. (2005) *J. Biol. Chem.* **280,** 16143–16150
10. Bednar, J., Horowitz, R. A., Grigoryev, S. A., Carruthers, L. M., Hansen, J. C., Koster, A. J., and Woodcock, C. L. (1998) *Proc. Natl. Acad. Sci. U. S. A.* **95,** 14173–14178
11. Zlatanova, J., Caiafa, P., and Van Holde, K. (2000) *FASEB J.* **14,** 1697–1704
12. Grummt, I., and Pikaard, C. S. (2003) *Nat. Rev. Mol. Cell. Biol.* **4,** 641–649
13. Fischle, W., Wang, Y., and Allis, C. D. (2003) *Curr. Opin. Cell Biol.* **15,** 172–183
14. Hebbes, T. R., Clayton, A. L., Thorne, A. W., and Crane-Robinson, C. (1994) *EMBO J.* **13,** 1823–1830
15. Lachner, M., O'Carroll, D., Rea, S., Mechtler, K., and Jenuwein, T. (2001) *Nature* **410,** 116–120
16. Fan, J. Y., Gordon, F., Luger, K., Hansen, J. C., and Tremethick, D. J. (2002) *Nat. Struct. Biol.* **9,** 172–176
17. McKittrick, E., Gafken, P. R., Ahmad, K., and Henikoff, S. (2004) *Proc. Natl. Acad. Sci. U. S. A.* **101,** 1525–1530
18. Mizuguchi, G., Shen, X., Landry, J., Wu, W. H., Sen, S., and Wu, C. (2004) *Science* **303,** 343–348
19. Sims, R. J., III, Mandal, S. S., and Reinberg, D. (2004) *Curr. Opin. Cell Biol.* **16,** 263–271
20. Haushalter, K. A., and Kadonaga, J. T. (2003) *Nat. Rev. Mol. Cell. Biol.* **4,** 613–620
21. Loyola, A., and Almouzni, G. (2004) *Biochim. Biophys. Acta* **1677,** 3–11
22. Tyler, J. K. (2002) *Eur. J. Biochem.* **269,** 2268–2274
23. Adams, C. R., and Kamakaka, R. T. (1999) *Curr. Opin. Genet. Dev.* **9,** 185–190
24. Ishimi, Y., Hirosumi, J., Sato, W., Sugasawa, K., Yokota, S., Hanaoka, F., and Yamada, M. (1984) *Eur. J. Biochem.* **142,** 431–439
25. Walter, P. P., Owen-Hughes, T. A., Cote, J., and Workman, J. L. (1995) *Mol. Cell. Biol.* **15,** 6178–6187
26. Chen, H., Li, B., and Workman, J. L. (1994) *EMBO J.* **13,** 380–390
27. Ohkuni, K., Shirahige, K., and Kikuchi, A. (2003) *Biochem. Biophys. Res. Commun.* **306,** 5–9
28. Park, Y. J., Chodaparambil, J. V., Bao, Y., McBryant, S. J., and Luger, K. (2005) *J. Biol. Chem.* **280,** 1817–1825
29. Redon, C., Pilch, D., Rogakou, E., Sedelnikova, O., Newrock, K., and Bonner, W. (2002) *Curr. Opin. Genet. Dev.* **12,** 162–169
30. Ito, T., Ikehara, T., Nakagawa, T., Kraus, W. L., and Muramatsu, M. (2000) *Genes Dev.* **14,** 1899–1907

31. Belotserkovskaya, R., Oh, S., Bondarenko, V. A., Orphanides, G., Studitsky, V. M., and Reinberg, D. (2003) *Science* **301,** 1090–1093
32. Orphanides, G., Wu, W. H., Lane, W. S., Hampsey, M., and Reinberg, D. (1999) *Nature* **400,** 284–288
33. Belotserkovskaya, R., Saunders, A., Lis, J. T., and Reinberg, D. (2004) *Biochim. Biophys. Acta* **1677,** 87–99
34. Levchenko, V., and Jackson, V. (2004) *Biochemistry* **43,** 2359–2372
35. Shintomi, K., Iwabuchi, M., Saeki, H., Ura, K., Kishimoto, T., and Ohsumi, K. (2005) *Proc. Natl. Acad. Sci. U. S. A.* **102,** 8210–8215
36. Ramos, I., Prado, A., Finn, R. M., Muga, A., and Ausio, J. (2005) *Biochemistry* **44,** 8274–8281
37. Ausio, J. (2000) *Biophys. Chem.* **86,** 141–153
38. Wang, X. Y., He, C., Moore, S. C., and Ausio, J. (2001) *J. Biol. Chem.* **276,** 12764–12768
39. Carruthers, L. M., and Hansen, J. C. (2000) *J. Biol. Chem.* **275,** 37285–37290
40. Dorigo, B., Schalch, T., Bystricky, K., and Richmond, T. J. (2003) *J. Mol. Biol.* **327,** 85–96
41. Hansen, J. C., and Turgeon, C. L. (1999) *Methods Mol. Biol.* **119,** 127–141
42. Hansen, J. C., Ausio, J., Stanik, V. H., and van Holde, K. E. (1989) *Biochemistry* **28,** 9129–9136
43. Carruthers, L. M., Schirf, V. R., Demeler, B., and Hansen, J. C. (2000) *Methods Enzymol.* **321,** 66–80
44. Garcia-Ramirez, M., Rocchini, C., and Ausio, J. (1995) *J. Biol. Chem.* **270,** 17923–17928
45. Schwarz, P. M., and Hansen, J. C. (1994) *J. Biol. Chem.* **269,** 16284–16289
46. Garcia-Ramirez, M., Dong, F., and Ausio, J. (1992) *J. Biol. Chem.* **267,** 19587–19595
47. Leuba, S. H., Yang, G., Robert, C., Samori, B., van Holde, K., Zlatanova, J., and Bustamante, C. (1994) *Proc. Natl. Acad. Sci. U. S. A.* **91,** 11621–11625
48. Zlatanova, J., Leuba, S. H., and van Holde, K. (1998) *Biophys. J.* **74,** 2554–2566
49. Leuba, S. H., Bustamante, C., van Holde, K., and Zlatanova, J. (1998) *Biophys. J.* **74,** 2830–2839
50. Leuba, S. H., Bustamante, C., Zlatanova, J., and van Holde, K. (1998) *Biophys. J.* **74,** 2823–2829
51. Yodh, J. G., Lyubchenko, Y. L., Shlyakhtenko, L. S., Woodbury, N., and Lohr, D. (1999) *Biochemistry* **38,** 15756–15763
52. Karymov, M. A., Tomschik, M., Leuba, S. H., Caiafa, P., and Zlatanova, J. (2001) *FASEB J.* **15,** 2631–2641
53. Bash, R., Wang, H., Yodh, J., Hager, G., Lindsay, S. M., and Lohr, D. (2003) *Biochemistry* **42,** 4681–4690
54. Wang, H., Bash, R., Yodh, J. G., Hager, G. L., Lohr, D., and Lindsay, S. M. (2002) *Biophys. J.* **83,** 3619–3625
55. Bash, R. C., Yodh, J., Lyubchenko, Y., Woodbury, N., and Lohr, D. (2001) *J. Biol. Chem.* **276,** 48362–48370
56. Yodh, J. G., Woodbury, N., Shlyakhtenko, L. S., Lyubchenko, Y. L., and Lohr, D. (2002) *Biochemistry* **41,** 3565–3574
57. d'Erme, M., Yang, G., Sheagly, E., Palitti, F., and Bustamante, C. (2001) *Biochemistry* **40,** 10947–10955
58. Giannasca, P. J., Horowitz, R. A., and Woodcock, C. L. (1993) *J. Cell Sci.* **105,** 551–561
59. Kepert, J. F., Fejes Tóth, K., Caudron, M., Mücke, N., Langowski, J., and Rippe, K. (2003) *Biophys. J.* **85,** 4012–4022
60. Fejes Tóth, K., Mazurkiewicz, J., and Rippe, K. (2005) *J. Biol. Chem.* **280,** 15690–15699
61. Lee, K. M., and Hayes, J. J. (1997) *Proc. Natl. Acad. Sci. U. S. A.* **94,** 8959–8964
62. Neben, K., Tews, B., Wrobel, G., Hahn, M., Kokocinski, F., Giesecke, C., Krause, U., Ho, A. D., Kramer, A., and Lichter, P. (2004) *Oncogene* **23,** 2379–2384
63. Laue, T. M., Shah, B. D., Ridgeway, T. M., and Pelletier, S. L. (1992) in *Analytical Ultracentrifugation in Biochemistry and Polymer Science* (Harding, S. E., Rowe, A. J., and Horton, J. C., eds) pp. 90–125, Royal Society of Chemistry, Cambridge, UK
64. Philo, J. S. (2000) *Anal. Biochem.* **279,** 151–163
65. Schuck, P. (2003) *Anal. Biochem.* **320,** 104–124
66. McBryant, S. J., Park, Y. J., Abernathy, S. M., Laybourn, P. J., Nyborg, J. K., and Luger, K. (2003) *J. Biol. Chem.* **278,** 44574–44583
67. Rivetti, C., and Codeluppi, S. (2001) *Ultramicroscopy* **87,** 55–66
68. Ausio, J., Borochov, N., Seger, D., and Eisenberg, H. (1984) *J. Mol. Biol.* **177,** 373–398
69. Sedat, J., and Manuelidis, L. (1978) *Cold Spring Harbor Symp. Quant. Biol.* **42,** 331–350
70. Belmont, A. S., and Bruce, K. (1994) *J. Cell Biol.* **127,** 287–302
71. Tumbar, T., Sudlow, G., and Belmont, A. S. (1999) *J. Cell Biol.* **145,** 1341–1354
72. Rivetti, C., Guthold, M., and Bustamante, C. (1996) *J. Mol. Biol.* **264,** 919–932
73. Kellogg, D. R., and Murray, A. W. (1995) *J. Cell Biol.* **130,** 675–685
74. Rabbani, A., Iskandar, M., and Ausio, J. (1999) *J. Biol. Chem.* **274,** 18401–18406
75. Zlatanova, J., and van Holde, K. (1996) *Prog. Nucleic Acids Res. Mol. Biol.* **52,** 217–259
76. Carruthers, L. M., Bednar, J., Woodcock, C. L., and Hansen, J. C. (1998) *Biochemistry* **37,** 14776–14787
77. Studitsky, V. M., Walter, W., Kireeva, M., Kashlev, M., and Felsenfeld, G. (2004) *Trends Biochem. Sci.* **29,** 127–135
78. Studitsky, V. M., Kassavetis, G. A., Geiduschek, E. P., and Felsenfeld, G. (1997) *Science* **278,** 1960–1963
79. Orphanides, G., LeRoy, G., Chang, C. H., Luse, D. S., and Reinberg, D. (1998) *Cell* **92,** 105–116
80. Orphanides, G., and Reinberg, D. (2000) *Nature* **407,** 471–475
81. Squazzo, S. L., Costa, P. J., Lindstrom, D. L., Kumer, K. E., Simic, R., Jennings, J. L., Link, A. J., Arndt, K. M., and Hartzog, G. A. (2002) *EMBO J.* **21,** 1764–1774
82. Nacheva, G. A., Guschin, D. Y., Preobrazhenskaya, O. V., Karpov, V. L., Ebralidse, K. K., and Mirzabekov, A. D. (1989) *Cell* **58,** 27–36
83. Hartzog, G. A., Speer, J. L., and Lindstrom, D. L. (2002) *Biochim. Biophys. Acta* **1577,** 276–286
84. Peng, H. F., and Jackson, V. (1997) *Biochemistry* **36,** 12371–12382
85. McQuibban, G. A., Commisso-Cappelli, C. N., and Lewis, P. N. (1998) *J. Biol. Chem.* **273,** 6582–6590
86. Misteli, T. (2001) *Science* **291,** 843–847
87. Zlatanova, J. (1990) *Trends Biochem. Sci.* **15,** 273–276
88. Crane-Robinson, C. (1999) *BioEssays* **21,** 367–371
89. Levchenko, V., Jackson, B., and Jackson, V. (2005) *Biochemistry* **44,** 5357–5372
90. Bruno, M., Flaus, A., Stockdale, C., Rencurel, C., Ferreira, H., and Owen-Hughes, T. (2003) *Mol. Cell* **12,** 1599–1606
91. Krogan, N. J., Dover, J., Wood, A., Schneider, J., Heidt, J., Boateng, M. A., Dean, K., Ryan, O. W., Golshani, A., Johnston, M., Greenblatt, J. F., and Shilatifard, A. (2003) *Mol. Cell* **11,** 721–729

Supplementary Figure S1

MNase digestions of different chromatin samples. Untreated chromatin isolated from HeLa cells showed a broadening of the bands, which is likely to represent the core nucleosome particle (cp) and the chromatosome (chr), i. e. a nucleosome with linker histone. The DNA component above the core particle disappeared completely upon histone H1 depletion resulting in an uniform protection of ~147 bp of DNA. Chromatin fibers with and without H1 were treated with NAP1 and showed a MNase pattern similar to the H1 depleted control chromatin. This provides further evidence for an extraction of H1 from chromatin by NAP1 and the integrity of the remaining core nucleosome particles. MNase incubation times are indicated in minutes. The DNA references lane (Ref) contains fragments of 100, 150 and 200 bp length. (**A**) MNase digestion of native HeLa chromatin. (**B**) MNase digestion of H1 depleted chromatin. (**C**) MNase digestion of NAP1 incubated chromatin. (**D**) MNase digestion of H1 stripped chromatin incubated with NAP1.
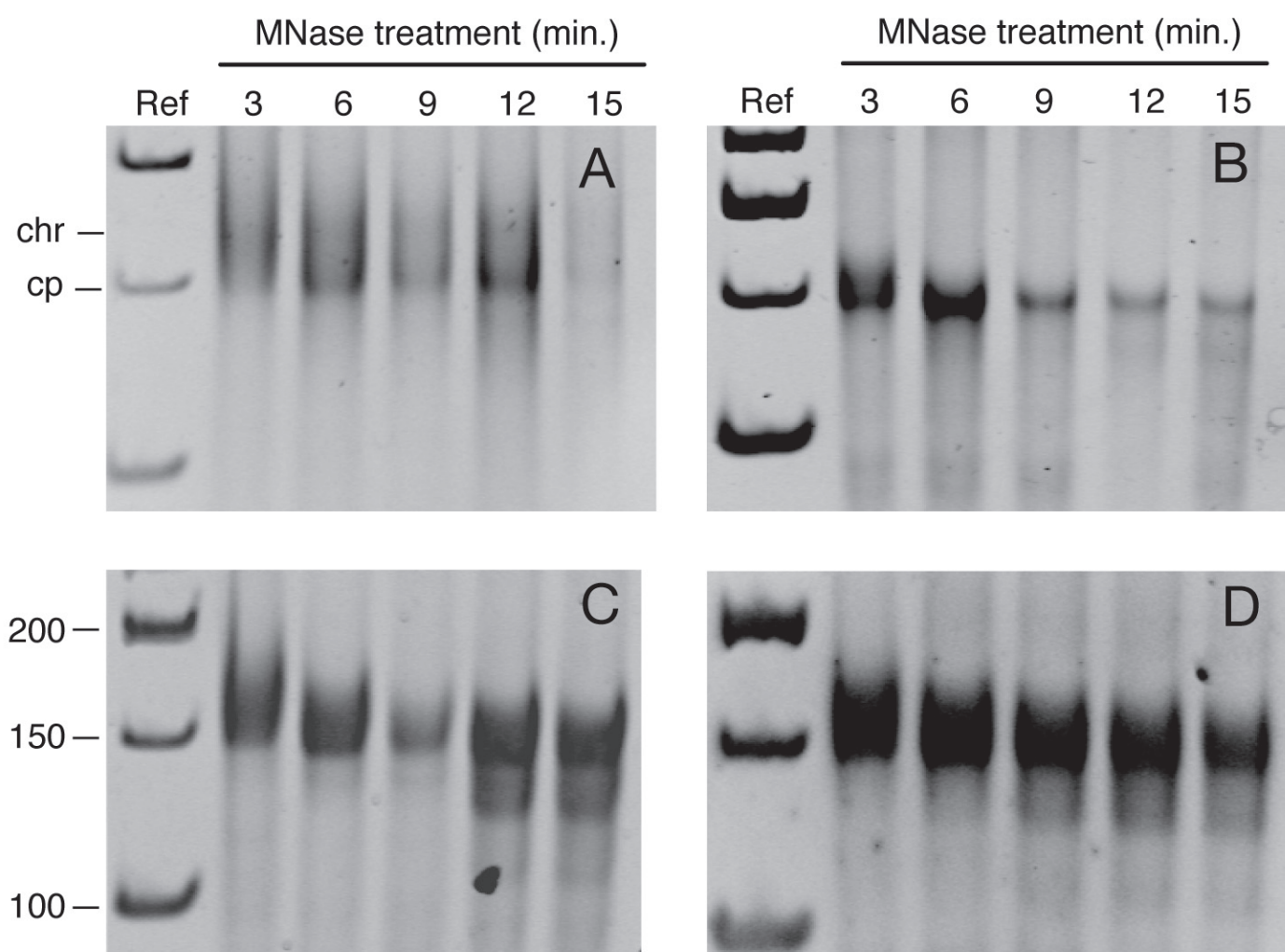
Supplementary Fig. S 1, Kepert et al.